4-1-1993

Monte Carlo Simulations of Water-Ice Layers on a Model Silver Iodide Substrate: A Comparison with Bulk Ice Systems

James H. Taylor

Barbara N. Hale
Missouri University of Science and Technology, bhale@mst.edu

Recommended Citation

J. H. Taylor and B. N. Hale, "Monte Carlo Simulations of Water-Ice Layers on a Model Silver Iodide Substrate: A Comparison with Bulk Ice Systems," *Physical Review B (Condensed Matter)*, vol. 47, no. 15, pp. 9732-9741, American Physical Society (APS), Apr 1993.
The definitive version is available at https://doi.org/10.1103/PhysRevB.47.9732

Monte Carlo simulations of water-ice layers on a model silver iodide substrate: A comparison with bulk ice systems

James H. Taylor* and Barbara N. Hale
Department of Physics and Center for Cloud Physics Research, University of Missouri-Rolla, Rolla, Missouri 65401
(Received 21 September 1992)

Two water layers adsorbed on a model silver iodide basal face are simulated at nine temperatures from 150 to 425 K using Monte Carlo methods. The periodic unit cell of 96 internally rigid water molecules (interacting via the revised central-force potentials) couples to the rigid-substrate atoms via effective pair potentials with Lennard-Jones short-range and Coulomb long-range terms. The distribution of molecules perpendicular to the substrate exhibits layering, and individual layer structure factors, dipole moments, and "pseudodiffusion" coefficients are calculated. A complex temperature dependence with the two layers taking on different solidlike, quasiliquid, or liquid properties at the same T is observed. Both layers appear to be solid at the lowest T studied. But for $T \geq 265$ K the upper layer becomes increasingly liquidlike with increasing T, whereas the lower layer of water molecules remains generally solidlike up to $T = 325$ K. Comparisons are made with constant number, volume, and temperature bulk ice Monte Carlo simulations and (flexible molecule) molecular-dynamics simulations using the same water-water potentials. Pseudodiffusion coefficients are compared with experimental values for ice, water, and with a quasiliquidlike layer of water on ice.

I. INTRODUCTION

The motivation for this work has been to study the processes by which ice nucleates on substrates. In particular, the interest lies in heterogeneous ice nucleation under atmospheric conditions. Effective ice nucleating agents have generally been classified by their threshold temperature (for ice formation) at water saturation. In general, the best substrates are those for which the lattice mismatch with ice is small. For example, hexagonal silver iodide (with a lattice mismatch of 2%–3%) was identified as an efficient ice nucleating agent some time ago.[1] However, classical theoretical models for heterogeneous nucleation rates[2–4] have had only moderate success. In some cases the nucleation rate predictions are as much as 14 orders of magnitude too large.[5] Other puzzling aspects of ice formation on (particulate) surfaces are the roles of substrate defects,[6–8] water-substrate bonding,[9,10] particulate (and the critical ice embryo) size,[11] and complications associated with liquidlike layers on the ice surface.[12–17] The present study is focused on the microscopic features of the first two monolayers of water molecules on a model basal face of hexagonal AgI. The goals have been to examine the structure and state (liquid versus solid) of the individual layers and to evaluate the applicability of classical heterogeneous nucleation rate formalisms for such a system.

A number of computer simulations have examined water in contact with model solid surfaces or walls.[18–31] Some of these studies focus on the water nonpolar solid interface[18–20,22] and some investigate model water-metal interfaces.[21,23–26,28,30,31] Many of the simulations use the 9-3 integrated Lennard-Jones potential with modifications representing hydrophobic, nonpolar[18–20,22] charged walls[22,25,26,30] and walls with image charges.[21] Other simulations incorporate specific structure into the wall[23,28,31] or investigate the effect of an electric field.[28] More realistic effective water-metal potentials have also been used.[23,27,28,31] Icelike structure in the water layers adjacent to the substrate have been reported.[20,22,31] Most of these studies use a symmetric configuration of water between two walls. In the present study we simulate two H_2O layers adsorbed on a model ice nucleating substrate with a free surface above the water layers (≈ 0 pressure in the vertical direction). In this configuration, characteristic of vapor to solid heterogeneous nucleation, the structure formation in the adsorbed water layers is greatly inhibited by the excess free surface entropy.

Earlier studies of water on model AgI surfaces (using effective atom-atom potentials) have examined optimal water monomer binding sites[32] and monolayer water clusters[33] on the defect-free basal and prism AgI faces, water monomer binding at point and extended (step) defects,[34] and critical cluster size (≈ 3 molecules) and nucleation rate ($\approx 10^{23}$ cm^{-2} sec^{-1}) for water monolayer formation on the basal face[35] at $T = 265$ K and water saturation. The latter work implies that the model AgI basal face (with water-substrate binding comparable to water-water binding) is rapidly covered with a solidlike water monolayer composed of six- (and some five-) membered ringe centered on the exposed iodine atoms. [Similar five- and six-membered ring structure is seen in small liquidlike monolayer water clusters on a smooth Lennard-Jones (9-3) surface.[36]] In order to examine the structure and state of additional water layers on the model AgI surface, the present work has been undertaken. Since no extensive studies of bulk ice *Ih* melting [using the same revised central-force potentials (RSL2) of Rahman and Stillinger[37,38]] have been available, companion constant volume, number, and temperature (NVT) Monte Carlo simulations of a model bulk ice *Ih* system (with corre-

sponding periodic boundary conditions, areal density, and intramolecular water molecule properties) have been carried out.[39,40] The goals of the latter work have been to provide an approximate melting-freezing temperature and temperature-dependent basal plane structure factors for the model ice *Ih* system.

The model system and simulation procedure are described in Sec. II, the results are given in Sec. III, and Sec. IV contains comments and conclusions.

II. THE MODEL SYSTEM AND MONTE CARLO SIMULATIONS

The constant area $[8(\frac{2}{3})^{1/2}R_0 \times 6(2)^{1/2}R_0]$ unit cell of 96 rigid water molecules is periodic parallel to the substrate. The intramolecular HOH angle and OH bond length are 101° and 0.972 Å, respectively, and $R_0 = 2.78$ Å. These values (found from a static energy minimization of 192 water molecules in the ice *Ih* configuration[39] using the same RSL2 potentials) allow comparison of the adsorbed water layer structure and state (liquid versus solid) with the model bulk ice *Ih* system simulated in the companion studies. The effective atomic electric charges, $q = 0.329\,83e$ and $-2q$, are fixed at the hydrogen and oxygen atomic positions, and give a molecular dipole moment of 1.96 D. This value is intermediate between the dipole moment in the vapor (≈ 1.86 D) and values estimated for ice (2–2.3 D).[10] A precalculated table of RSL2 water-water potential values is used in the simulations and a cutoff at 6 Å (based on the oxygen-oxygen separation distance) is assumed to reduce computer time.

A model rigid iodine-exposed basal face of silver iodide in a wurtzite structure (with lattice constants $a = 4.58$ Å and $c = 7.49$ Å) serves as the substrate. The water-substrate interaction contains three terms: a 6-12 Lennard-Jones term V_{LJ}, a Coulomb term V_{el} (assuming $0.4e$ and $-0.4e$ effective substrate atomic charges[33]), and an induced polarization term V_{ind}.[34] These are described in more detail in the Appendix. Four separate three-dimensional water-substrate potential grids for the Lennard-Jones, the Coulomb interaction, and the inductive interactions are generated using an Ewald sum for the Coulombic terms[32,41] and a cutoff of 15 Å for the remaining terms. Linear interpolation between grid points is used to evaluate the water-substrate interaction during the Monte Carlo simulations. Additional constraints on the water-substrate interaction are a hard wall at 1 Å above the $z = 0$ plane of exposed iodine atoms (to prevent penetration of the substrate by water molecules) and a cutoff at $z = 20$ Å. In the simulations, most of the molecules remain above $z = 2.0$ Å and no molecules reach $z > 15$ Å.[42]

The Metropolis[43] Monte Carlo (MC) simulations execute three independent translations along the Cartesian axes and a rotation (with maximum value ≈ 0.05 rad) about a randomly chosen Cartesian axis at each step using a total of six random numbers. Maximum displacements during the runs are as described below. Simulations are performed at nine temperatures: 150, 200, 230, 265, 285, 300, 325, 375, and 425 K. We note that layering in fluids adjacent to substrates is well known[22,26,44,45] and the present system also exhibits layering. In order to monitor independently quantities for an upper (free surface) layer and a lower (adjacent to the substrate) layer, an artificial plane boundary between layers is assumed (with respect to oxygen positions) at $z = 3.2$ Å; the substrate plane is located at $z = 0$ Å. The latter layer definition is consistent with the observed layering and allows instantaneous assignment of molecules to the upper or lower layer. In these simulations we calculate average layer specific values for the dipole moments, structure factors, and root-mean-square oxygen displacements. Though molecules are free to cross this boundary, the numbers in the individual layers are found to be nearly stable. During equilibration runs, the layering is used to introduce a 90% preferential sampling of molecules in the upper layer. A correction factor in the acceptance criterion to prevent the artificial accumulation of molecules in the lower layer is used.[46] This enhances (reduces) the probability of travel from the lower (upper) layer. The multiplicative correction factor P_c is given by

$$P_c = n_a/9(n_b+1) \quad \text{(from upper to lower layer)}, \tag{2.1a}$$

$$P_c = 9n_b/(n_a+1) \quad \text{(from lower to upper layer)}, \tag{2.1b}$$

$$P_c = 1 \quad \text{(no layer transition)}, \tag{2.1c}$$

where n_a (n_b) is the number of molecules above (below) the lower-layer boundary before the trial move.

The initial water molecule configurations for the simulations reported in this work are generated as follows. A 192-molecule, four-layer unit cell (48 molecules per layer) of ideal ice *Ih* (Ref. 39) is placed 3 Å above the AgI substrate with basal faces parallel and with six-membered rings in the ice structure centered on the exposed iodines. This system is then run at $T = 1000$ K for 10^5 MC steps using the above-described unit-cell boundary conditions. Next, the 96 water molecules farthest from the substrate are removed. Finally a MC simulation is made for $N_i = 7 \times 10^6(7M)$ MC steps at 200 K using normal sampling and a maximum displacement of 0.01 Å. This final configuration is used as an initial configuration for further MC equilibrating simulations (with N_e steps) followed by N_a averaging steps. Data collection simulations of length N_a are performed using normal importance sampling and maximum displacements adjusted to give an acceptance ratio ≈ 0.5. See Table I. The simulations required ≈ 3.5 h per million steps on an Amdahl V7. A slight spreading of the (intramolecular) HOH angle ($\leq 0.2\%$) and OH bond length ($\leq 0.6\%$) from round-off during the large number of center-of-mass rotations is noted.

The 0.904 g/cm^3 bulk ice *Ih* NVT Monte Carlo simulations[39,40] (with which the present results are compared) used periodic unit cells of 192 rigid water molecules (4 crinkled layers of 48 molecules each) with cell dimensions $[8(\frac{2}{3})^{1/2}R_0 \times 6(2)^{1/2}R_0 \times \frac{16}{3}R_0]$. The R_0, intramolecular parameters, and water-water potentials were identical to those used in the present simulation. The intermolecular potentials[37] were calculated directly with a cutoff of 5 Å. Simulations for the model bulk ice system with a cutoff of 6 Å gave similar results near the liquid-solid coexistence

TABLE I. Equilibration information and results for average interaction energies per molecule for the adsorbed layers. Numbers of MC steps are in millions. N_i is the step number at which the initial configuration was taken from the initializing run, N_e is the number of equilibration steps, and N_a is the number of data collection steps. Average potential energies U and their standard deviations are in kcal/mol per molecule. U_T is the total potential energy, U_{int} is the intermolecular energy, and U_s is the water surface interaction energy. Standard deviations are found from the fluctuations in the given quantity. $C=[\langle U_T^2\rangle-\langle U_T\rangle^2]/kT^2+0.33$, and is roughly equal to the specific heat at constant volume, in units of cal/(g K). The additive factor of 0.33 is the kinetic-energy contribution.

T	N_i	N_e	N_a	$-U_T$	$-U_{\text{int}}$	$-U_s$	C
150	0.00	4.10	2.00	13.08±0.06	9.64±0.06	3.44±0.04	0.72
200	7.11	6.06	2.00	12.67±0.08	9.27±0.08	3.40±0.05	0.72
230	0.00	4.10	2.00	12.50±0.11	9.12±0.10	3.38±0.04	0.89
265	0.00	4.10	5.00	12.21±0.14	8.89±0.14	3.31±0.06	1.10
285	0.00	1.00	9.00	12.19±0.15	8.83±0.14	3.36±0.06	1.05
300	0.00	4.30	5.00	11.78±0.15	8.51±0.14	3.26±0.07	1.00
325	0.00	4.30	5.00	11.53±0.20	8.31±0.18	3.22±0.07	1.30
375	0.00	4.30	2.00	10.86±0.15	7.68±0.15	3.18±0.07	0.78
425	0.00	5.40	2.00	9.87±0.21	6.88±0.18	2.98±0.09	0.96

region. The molecular-dynamics simulations of model bulk ice *Ih*,[47] assumed the same unit-cell dimensions, but flexible water molecules using the same RSL2 water-water potential.[37]

III. RESULTS

In all the simulations the following quantities are monitored: the dipole moment $\mathbf{p}$ and $|\mathbf{p}|$ for a given layer, the structure factors per molecule, S_i (for the $\mathbf{k}_i$ basal face reciprocal-lattice vector) in a given layer, the intermolecular potential energy per molecule, U_{int}, the water-substrate potential energy per molecule, U_s, the squares of these energies, and the distribution of molecules in constant z planes above the substrate, $\rho(z)$. The calculated values are given in Tables I and II and general results are described below.

A. The intermolecular, substrate, and total potential energies

Both the average water-substrate and intermolecular potential energies generally increase with increasing temperature. The fluctuations in the energies are all less than about 3% of their magnitudes, but generally increase in

TABLE II. Results for the water layer system where 1 (2) denotes the lower (upper) layer. Dipole moments are in e Å, where 1 e Å=4.8 D, and are for the entire layer. Structure factors are per molecule. Because of variations in the number of molecules in a layer, the dipole moments and structure factors given below are good to within about 3%. Root-mean-square displacements R_L and R are in Å. R_L is given separately for top and bottom layers. Note that R_L and R are for different numbers of steps and R is for both layers.

System / Water layer	T	$\langle P_x\rangle$	$\langle P_y\rangle$	$\langle P_z\rangle$	$\langle P\rangle$	$\langle S_1\rangle$	$\langle S_2\rangle$	R_L	R
1	150	−0.41	−0.61	−0.62	1.1	0.44	0.44	0.30	0.45
2		−2.00	1.30	−3.70	4.4	<0.1	0.03	0.53	
1	200	−0.57	−0.42	−0.51	1.0	0.45	0.43	0.37	0.74
2		−0.40	−0.26	−3.20	3.3	0.01	0.05	0.90	
1	230	0.55	−0.43	0.14	1.0	0.44	0.52	0.46	0.75
2		−0.27	−0.61	−3.50	3.7	0.04	0.04	0.92	
1	265	0.57	−0.50	−0.20	1.1	0.41	0.47	0.54	1.14
2		0.01	1.40	−2.80	3.3	0.04	0.02	1.41	
1	285	0.44	−1.70	−0.49	2.0	0.56	0.50	0.65	1.35
2		0.38	1.20	−3.20	3.7	0.10	0.10	1.70	
1	300	−0.93	−0.63	−0.24	1.4	0.55	0.51	0.96	1.50
2		1.70	−0.85	−2.70	3.6	0.04	0.03	1.80	
1	325	−0.45	0.30	−0.20	1.2	0.45	0.45	1.01	2.15
2		0.04	−0.02	−2.50	2.9	0.03	0.05	2.66	
1	375	0.21	−2.40	−0.81	3.0	0.48	0.41	1.06	1.92
2		−1.50	0.95	−2.40	3.4	0.04	0.02	2.31	
1	425	−0.15	−0.07	−1.00	1.6	0.40	0.38	1.33	3.14
2		−0.15	0.17	−1.90	2.8	0.03	0.03	3.77	

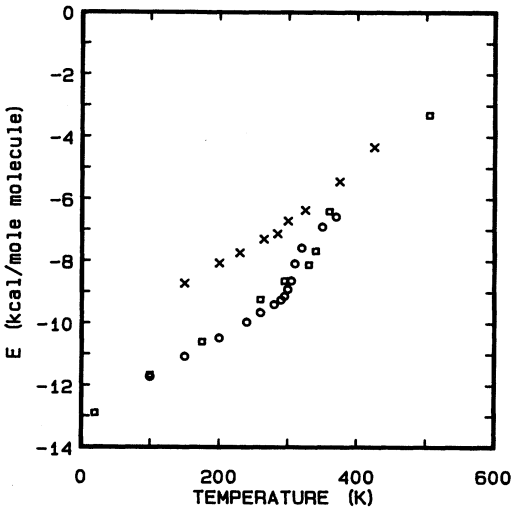

FIG. 1. The kinetic plus water-water interaction potential energy per molecule for the two water layer systems on the basal AgI substrate and for the bulk ice/water systems. Open circles represent the bulk Monte Carlo simulation (Ref. 40), open squares represent the bulk molecular-dynamics simulation (Ref. 47), and ×'s represent the two-layer system on the model basal AgI substrate.

relative size with increasing temperature. The sum of the average kinetic and intermolecular potential energies per molecule versus temperature (Fig. 1) appears to lie on two straight lines with the intersection occurring near 300 K. This latter change in slope suggests a phase change and will be discussed further below, in connection with other properties of the system. In Fig. 1 is also plotted the total energy per molecule for the bulk ice NVT systems.[40,47] We note that the Monte Carlo constant volume pressure versus temperature results of Han and Hale[40] show the onset of liquid-solid coexistence between 280 and 290 K.

The total energies remain quite stable throughout the averaging runs. Small anomalies did occur during the equilibrating runs, however. One of the problems with such simulations (particularly for water near a phase transition) is the verification of equilibration.

B. Structure factors and distribution of molecules above the substrate

The reciprocal-lattice vectors for the structure factors S_i are

$$\mathbf{k}_i=(\tfrac{2}{3})^{1/2}R_0[\hat{\mathbf{x}}+(-1)^i 3^{(-1/2)}\hat{\mathbf{y}}]\ ,$$

where $i=1,2$.[48] These two-dimensional structure factors reflect the match between the xy projections of the oxygen coordinates and the perfect basal face ice *Ih* structure. We note that layer boundary crossings introduce small discontinuities in the structure factors as functions of MC step and a 2%–3% uncertainty in the average "layer" structure factors per molecule.

Another indicator of structure is $\rho(z)$, the average

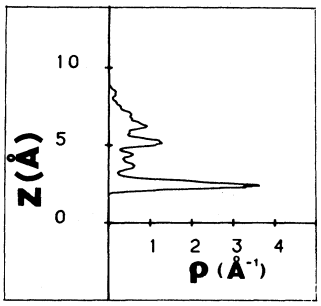

FIG. 2. The distribution of molecules perpendicular to the substrate, $\rho(z)$, for $T=200$ K, where ρ has units (0.1 molecules/Å). The $z=0$ Å plane passes through the exposed I atoms.

number of molecules in 0.05-Å bins centered on equally spaced values of z, starting at $z=1$ Å. In the ice *Ih* structure, the "layers" (parallel to the basal face) are composed of crinkled six-membered rings whose molecules lie alternately $R_0/6$ above and below the mean molecular plane. This has the effect of forming double layers of molecules or, equivalently, double peaks in $\rho(z)$ separated by approximately $R_0/3=0.93$ Å. Figure 2 shows $\rho(z)$ at $T=200$ K. This is typical of most temperatures. While layering (as generally expected for a liquid near a solid surface) is evident, there is little evidence of double peaks. One possible explanation for the single-peak structure of the lower layer is a water-substrate binding energy too large to allow the molecules to relax into crinkled rings. Figure 3 shows snapshots of the water molecules in the lower and upper layers at 200 K. Three configurations (separated by approximately 1 million MC steps) are superimposed to indicate the extent of

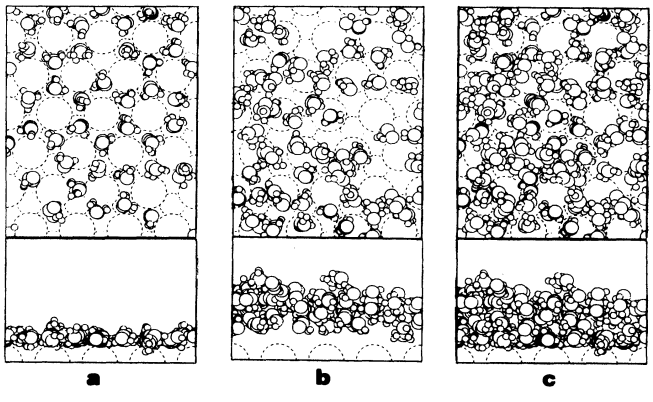

FIG. 3. Views of the 96 water molecule unit cell for the two-layer system on the basal AgI face at 200 K showing (a) the lower layer, (b) the upper layer, and (c) both layers. In each view three configurations separated by approximately one million steps are superimposed to indicate the extent of thermal motion. The top view is along $-\hat{\mathbf{z}}$ and the bottom view is parallel to the AgI surface; Ag (I) atoms are shown as small (large) dashed circles and H (O) atoms are shown as small (large) solid circles.

thermal motion. Note the solidlike six-membered ring structure in the lower layer and the less-stable disordered molecular arrangements in the upper layer.

Figure 4 shows $(S_1+S_2)/2$, the average structure factor for a given layer as a function of temperature. The average structure factor in the upper layer is small at all T and comparable to the 350-K bulk structure factors. This lack of structure is expected for high temperatures. At lower T it suggests the existence of an amorphous solid or a liquidlike layer, consistent with experimental evidence for a quasiliquid layer[12-17] on ice at temperatures close to the melting point. At the lowest temperatures (230, 200, and 150 K), the molecules have probably been frozen into a disordered state which emerged during the initialization of the water layer system. This will be discussed later in terms of molecular diffusion. At intermediate temperatures, however, the molecules in the upper layer should have sufficient kinetic energy to reorder.

The structure factors per molecule for the lower layer are comparable to those for bulk ice at 260 K. This is surprising at the higher temperatures (above 325 K) but near 300 K is consistent with infrared absorption experiments which indicate the presence of ice structure above the melting temperature in thin layers of water on silver iodide.[49] (There is also experimental evidence for the persistence of order in previously frozen water monolayers on some substrates, if the sample is not heated excessively.[50,51])

Examination of the more detailed temperature dependence of the average structure factor for the lower layer indicates an overall increase with temperature up to 285 K, probably because of defect annealing. Also, there is a slow decrease for T greater than 285 K, and a definite drop above 375 K. A short run at 500 K produces a further drop to 0.33 and indicates the expected tendency for desorption. From the present work it is only possible to predict a melting temperature for the lower layer between 300 and 375 K—probably near 325 K.

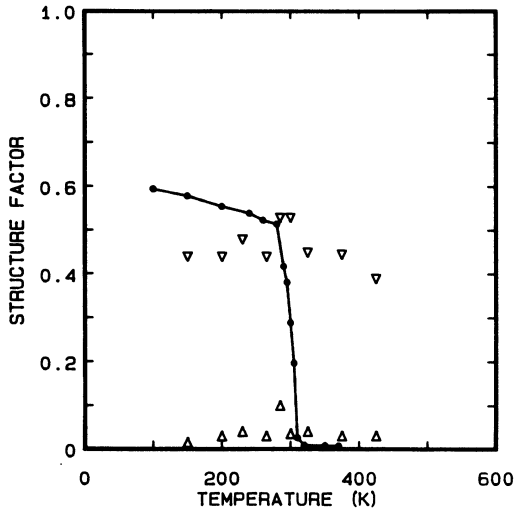

FIG. 4. The average structure factor, $S=(S_1+S_2)/2$ for ice basal face lattice vectors versus temperature for the bulk ice Monte Carlo simulation (Ref. 40) (solid circles), the upper water layer on AgI (open triangles), and the lower water layer on AgI (inverted open triangles). Straight lines connect the points for the model bulk ice data.

C. Dipole moments per layer

At all temperatures the magnitude of the total dipole moment (for a layer of about 48 water molecules) is small. See Fig. 5. The p_x and p_y show some cancellation between layers, and no preferred orientation. The p_z for both layers is directed toward the substrate. However, the lower layer has a small p_z consistent with the equilibrated bulk-ice values, whereas the upper-layer molecules have a distinct polarization along $-z$. The lower-layer ring structure appears to preferentially orient the dipole moments parallel to the substrate. See Fig. 3. On the other hand, the upper-layer molecules are free to respond more readily to the electrostatic interaction with the exposed layer of negative iodide ions. One cannot conclude anything from the present study about the dipole orientation at a vapor-liquid water interface[52,53] in the absence of a substrate.

D. Specific heats

The specific heats are calculated in two ways: from the fluctuations in the total potential energy of the system, $C=(\langle U^2\rangle-\langle U\rangle^2)/k_BT^2+3k_B$ (where k_B is the Boltzmann constant and U is the intermolecular potential energy) and from the slope of the total (intermolecular plus kinetic) energy versus temperature. See Table I for the specific heat C from the first method.

The $3k_B$ contribution to C from the kinetic energy comprises 20%–40% of the total specific heat. The C values are plotted in Fig. 6—together with C values for the bulk ice system from the Monte Carlo simulation.[40] The specific heat for the adsorbed two water layer system shows a general increase with T up to about 265 K, then a decline to about 300 K. The values at 325, 375, and 425 K show fluctuations which remain unexplained. The possibilities of nonequilibration and/or overlapping (and different) changes of state in the two layers as a function of temperature complicate the situation. For example, in the lower layer near 325 K melting is likely. In the upper layer near 375 K desorption is likely. The values of C at $T=150$ and 200 K are comparable to those of the bulk ice system, whereas the value of C for 265, 285, and 300 K are closer to the liquid water value at 350 K.

In the second method the specific heat is calculated from the slope of the energy vs T curve in Fig. 1. The values are $\approx 0.7\pm0.1$ cal/g K for $T\leq 265$ K and 1.1 ± 0.2 cal/g K for $T\geq 325$ K. These values are close to those for the Monte Carlo bulk simulation[40] and the molecular-dynamics simulation (1.03 cal/g K for the liquid and 0.66 cal/g K for the solid systems).[47] In the present simulation the energy value at 285 K cannot be placed conclusively on either line and has been excluded from the calculation of the slopes.

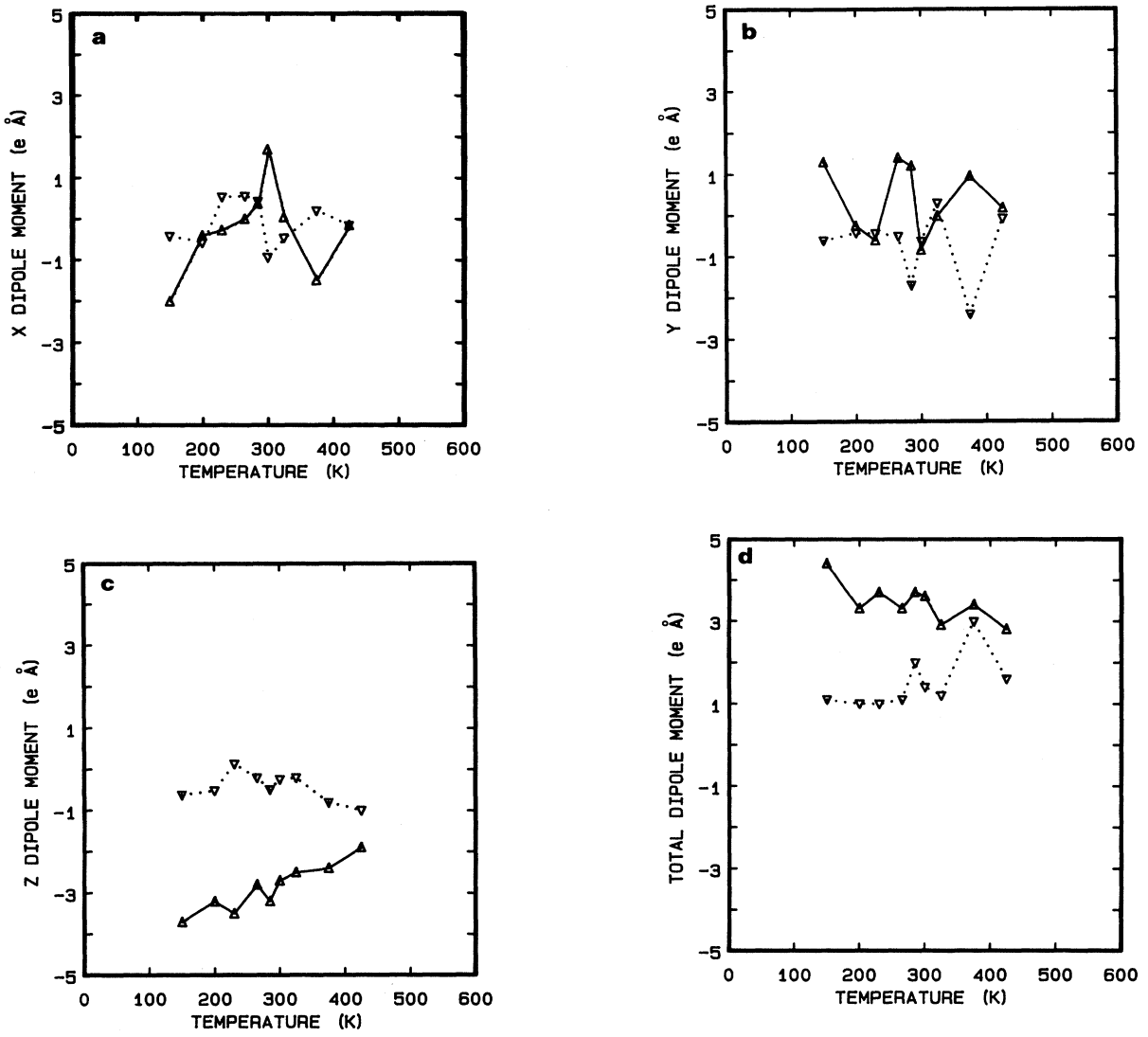

FIG. 5. The dipole moment of the upper layer of approximately 53 water molecules (open triangles) and the lower layer of approximately 43 water molecules (inverted open triangles) in the two water layer system on the model basal AgI substrate: (a) the x component, (b) the y component, (c) the z component, and (d) the magnitude of the dipole moment. Straight lines connect the points. In the vapor, one water molecule has a dipole moment equal to approximately 1.86 D=0.38 e Å; in the water layer system each molecule has a dipole moment of 1.96 D.

E. Pseudodiffusion coefficients

During the simulations, the distance of each oxygen from its original position, the mean-square displacement of each oxygen per move (rather than per step), MSDM, and the total number of moves for each oxygen are monitored. From these quantities, a mean-square displacement for a given layer, $\langle \mathrm{MSD}_i \rangle$, at any step number can be approximated by noting which molecules are in the layer at a given step and averaging (over those molecules) the MSDM. The normal procedures for calculating a mean-square displacement for a given layer cannot be used since a few molecules "diffuse" between layers during the run.

After a sufficient number of steps the $\langle \mathrm{MSD}_i \rangle$ stabilize and exhibit one of the following properties versus step number: (1) a very small slope (indicating a solidlike state); (2) a slope which increases moderately with step number (indicating a quasiliquid or liquidlike state); or (3) a much larger slope (indicating a real liquid or quasivapor state). As expected all the slopes for the upper layer are at least an order of magnitude larger than for the lower layer at the same temperature. In the lower-(upper-) layer case (1) occurs for $T \leq 265$ (230) K. For both layers at 375 and 425 K the slope is large [case (3)]. At intermediate temperatures case (2) holds. The slope of the stabilized $\langle \mathrm{MSD}_i \rangle$ versus step number per molecule, $\langle \delta \mathrm{MSD}_i \rangle / \delta N$, is used for determine a "pseudodiffusion" coefficient (in Å^2/step) for the ith layer, D_i:

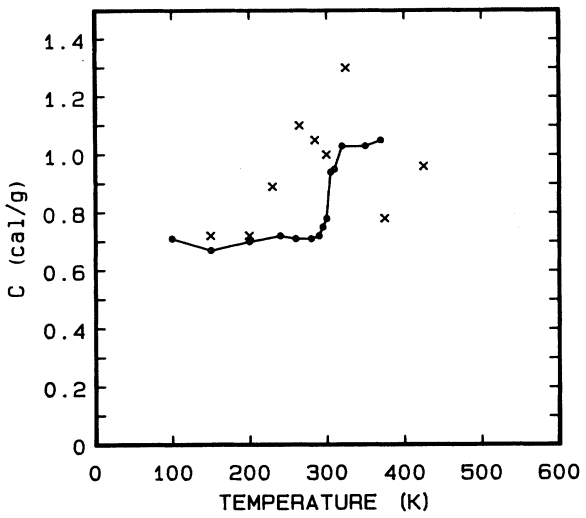

FIG. 6. Specific heat C vs temperature for the two-layer system on AgI ($\times$) and the bulk ice/water system (Ref. 40) (circles) calculated from the fluctuations in the total energy of the system. Straight lines connect the bulk ice points. The constant density bulk ice system enters a liquid-solid coexistence region near 280 K and does not have a "peak" in the specific heat at the boundary.

$$D_i = \langle \delta \mathrm{MSD}_i \rangle / (6\delta N) \, . \tag{3.1}$$

The D_i give a rough measure of the relative mobility of the molecules.[54] Obviously, real diffusion does not occur in Monte Carlo simulations.

An approximate conversion factor of 10^{15} steps/sec is obtained by relating the Monte Carlo[40] and molecular-dynamics[47,55] results for similar bulk systems. The self-diffusion coefficient from the molecular-dynamics simulation at 330 K, where $D \approx 0.7$ cm^2/sec, is compared to the slope of the root-mean-square displacement versus the number of steps per molecule in the Monte Carlo simulations at 350 and 320 K. The D_i, in units of cm^2/sec, are shown in Fig. 7. These "pseudodiffusion" coefficients for the water layers are compared with experimental values of the self-diffusion coefficient for liquid water,[56] natural single-crystal ice,[57] a "quasiliquid layer" on ice,[15] a melted bulk ice Monte Carlo simulation at 350 K,[40] the melting bulk ice flexible molecular-dynamics simulation at 330 K,[47,55] and a molecular-dynamics simulation for liquid water by Stillinger and Rahman[37] using the RSL2 water-water potentials with density $=1$ g/cm^3.

It is not clear whether the same conversion between steps and seconds has meaning for the adsorbed water layers. However, assuming the conversion is correct to within an order of magnitude, the pseudodiffusion coefficients for the adsorbed water layers fall distinctly below the experimental values for liquid water and above the experimental values for ice. Such a rough conversion between steps and seconds also places the adsorbed water layer pseudodiffusion coefficients above those observed for a "quasiliquid layer" obtained from the nuclear magnetic resonance studies of Mizuno and Hanfusa.[15]

One unsatisfactory feature of the water layer D values

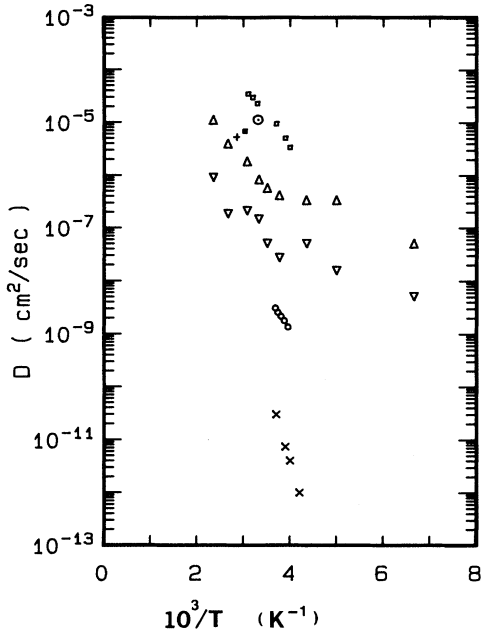

FIG. 7. Temperature dependence of the pseudodiffusion coefficients from Monte Carlo simulations (in cm^2/sec) for the upper layer of water on AgI (open triangles), lower layer (inverted triangles), and bulk H_2O NVT simulation (Ref. 40) (+). Also shown are the self-diffusion coefficients from: 1 g/cm^3 liquid water molecular-dynamics simulations using the RSL2 potential (Ref. 37) ($\odot$); the 0.904 g/cm^3 molecular-dynamics simulations using the RSL2 potentials (Refs. 47 and 55) (solid square); experimental values for liquid water (Ref. 56) (open squares), ice (Ref. 57) ($\times$), and a "quasiliquid layer" on ice (Ref. 15) (open circles). The conversion 10^{15} Monte Carlo steps equal to 1 sec is used.

remains. The values for the lower layer (which appears in all other respects to be solidlike at temperatures below 325 K) are large compared to those for solid bulk ice. A possible explanation is that the water layer adjacent to the substrate (defined to be below 3.2 Å) contains several molecules (perhaps of the order of 10%) which diffuse readily out of and back into the lower layer. Also, the lower layer probably contains more "defects" than bulk ice. A third possibility is that the molecules in the lower layer acquire enhanced diffusion because of the adjacent liquidlike layer. It should be pointed out that an order-of-magnitude decrease in the conversion factor (to 10^{14} steps/sec) for the water layers would yield rough equality between the lower-layer results and those for the quasiliquid layer. A two-order-of-magnitude adjustment would bring the upper-layer values down to those for the quasiliquid layer and the lower-layer values close to those of bulk ice. While this seems plausible from a physical point of view, it is not possible to justify such a low conversion factor from the available simulational data. In any case, it is clear that the plot of the pseudodiffusion coefficients versus $1/T$ shows a change in slope between 230 and 285 K for both layers—indicating a shift in the diffusion barriers. Diffusion barriers calculated from the

pseudodiffusion coefficients at higher temperatures (for both layers) appear to be closer to that for liquid water (4.5 kcal/mol) than for ice (≈ 15 kcal/mol).

IV. DISCUSSION OF RESULTS

At all the temperatures up to 375 K the model (iodine exposed) basal face of AgI appears to order the lower water monolayer in a solidlike plane of five- and six-membered rings centered on the iodines. The structure factor results suggest that this layer begins to disorder between 300 and 325 K. The pseudodiffusion coefficient data in this temperature region are not inconsistent with this picture. The existence of an ordered layer at temperatures above the apparent model bulk ice melting temperature (near 280 K)[40] is consistent with the experimental finding of Bakhanova and Kiselev,[49] who observed an "icelike" infrared absorption band for a thin film of H_2O on AgI at temperatures from 264 to 293 K. For all the temperatures studied, the ice basal face structure factors of this lower layer are comparable to those in the model bulk ice system. At $T=285$ and 300 K the lower-layer structure factor per molecule shows a distinct peak—possibly due to the annealing out of previously frozen defects. The peak gives further indication that this layer is solidlike at 300 K. The pseudodiffusion coefficients for the lower layer are large compared to the experimental values for bulk ice. This could be due to the liquidlike properties of the neighboring upper layer or to annealing effects. The lower monolayer has a nearly zero dipole moment projection perpendicular to the substrate.

In the present simulations for $T \leq 230$ K the upper layer displays properties similar to those of an amorphous solid; the large number of defects at the surface probably gives rise to the rather large pseudodiffusion coefficient. For $T \geq 265$ K, the upper layer displays more liquidlike properties. First, the structure factors are similar to those for liquid water. Second, the diffusion barrier (≈ 3 kcal/mol) is similar to that for liquid water (4.5 kcal/mol). Third, the pseudodiffusion coefficient is only about one order of magnitude smaller than that found experimentally for liquid water.[56] The existence of liquidlike surface layers and/or surface premelting effects has been indicated on surfaces other than ice.[58–60] For example, the effect of surface melting has been observed at the (110) surface of lead.[61] Computer simulations have also examined surface premelting phenomena.[62–67] In particular, it appears that diffusion coefficients and small diffusion barriers alone are not sufficient to determine the state of the surface layer. Finally, the upper layer of water has a net dipole moment directed into the substrate—probably arising from the exposed iodine surface charge.

Not surprisingly, the system seems to be "evaporating" for $T \geq 375$ K, with upper-layer molecules rising off the surface 10 Å or more, and those in the lower layer working their way into the upper layer. The mean-square displacements for both layers also show a steady increase with step number above 375 K. Over this range of temperature, there is a consistent decline in the structure factors and/or molecule of both layers, the more marked in the lower layer because of its relatively high initial values. A short simulation at 500 K corroborates this, with structure factors and/or molecule dropping to less than 0.33 in the lower layer in less than three million steps (equilibration run included), and molecules rapidly leaving both layers.

V. CONCLUSIONS AND COMMENTS

The simulations indicate that the model adsorbed water system takes on a complex character with the upper and lower layers displaying different solidlike, quasiliquid, or liquid properties at the same T. The implications of this for theories of ice nucleation on AgI and other substrates could be significant. Clearly the model of a simple spherical cap of ice on an undistorted basal face of AgI would not describe this system.

Some experimental studies have reported that ice does not form readily on the basal face of AgI.[68] The present study indicates that at least in the second adsorbed layer ice formation above about 265 K is inhibited by the free surface entropy. It should be noted that the conclusions of the present work cannot be applied to the prism face of AgI. Our previous work with models for water on the AgI prism face indicates that the first water monolayer is even less structured than on the basal AgI face. Possible remedies to this difficult situation for ice formation on AgI are not lacking. The popular view is that impurities (probably steps and ledges) play a large role in stabilizing the water molecules. Some preliminary simulations for two water layers on a model basal face ledge indicate that the ledge is marginally better at promoting ice structure in the upper layer.

An interesting possibility is that ice nucleation occurs within a thicker film of adsorbed water on the basal AgI face after the two-dimensional nucleation of a solidlike monolayer adjacent to the substrate. The three-dimensional nucleation would then occur on the icelike underlayer with an extremely small lattice mismatch.

ACKNOWLEDGMENTS

This work was supported in part by the National Science Foundation under Grants No. ATM83-10854 and No. ATM87-13872.

APPENDIX

The water-substrate interaction given below is the same as that used in Ref. 34, except that here a three-point-charge model of the water molecule is used, instead of the four-point-charge model used there:

$$V_{\mathrm{LJ}}=\sum_m 4\epsilon_{mw}\{(\sigma_{mw}/|\mathbf{r}_0-\mathbf{r}_m|)^{12}-(\sigma_{mw}/|\mathbf{r}_0-\mathbf{r}_m|)^6\}\ , \tag{A1}$$

$$v_{\mathrm{el}}=\tfrac{1}{2}\sum_{i,m} q_i q_m/|\mathbf{r}_i-\mathbf{r}_m|\ , \tag{A2}$$

$$v_{\text{ind}} = -\tfrac{1}{2}\sum_{n,m} \alpha_w q_n q_m (\mathbf{r}_0-\mathbf{r}_n)\cdot(\mathbf{r}_0-\mathbf{r}_m)/[|\mathbf{r}_0-\mathbf{r}_n||\mathbf{r}_0-\mathbf{r}_m|]^3 - \tfrac{1}{2}\sum_{n,i,j} \alpha_n q_i q_j (\mathbf{r}_i-\mathbf{r}_n)\cdot(\mathbf{r}_j-\mathbf{r}_n)/[|\mathbf{r}_i-\mathbf{r}_n||\mathbf{r}_j-\mathbf{r}_n|]^3 , \quad \text{(A3)}$$

where n and m indicate substrate ions and i and j the individual charges in the water molecule. The q_n, α_n, and $\mathbf{r}_n$ are the effective charge, polarizability, and position vector of the nth atom in the substrate, respectively. The q_i, α_w, and $\mathbf{r}_0$ are the atomic charges, polarizability, and center-of-mass position vector of the water molecule, respectively. The values of the parameters in the potential functions are $\sigma_{Agw}=3.171$ Å, $\epsilon_{Agw}=0.5467$ kcal/mol, $\sigma_{Iw}=3.342$ Å, $\epsilon_{Iw}=0.622$ kcal/mol, $\alpha_{Ag}=2.4$ Å^3, $\alpha_I=6.43$ Å^3, and $\alpha_w=1.44$ Å^3. The position vectors r have units of Å. The potential functions have units of kcal/mol.

Since in the first inductive term cancellations occur when $n\neq m$, only the $n=m$ terms are included in the generation of the grid. In the grid for the second inductive term (the contribution from polarization of the substrate atoms) the water molecule has its dipole moment directed perpendicular to the substrate along $+\hat{\mathbf{z}}$. The interpolation from this grid is multiplied by $[1+(\mathbf{p}\cdot\hat{\mathbf{z}}/p)^2]/2$ where $\mathbf{p}$ is the water molecule dipole moment. Beyond 5 Å the potential is essentially uniform in planes of constant z and a five-point Lagrange interpolation is used in the z direction. For oxygen-substrate distances greater than 10 Å, the potential is set equal to zero.

*Present address: Department of Physics, Central Missouri State University, Warrensburg, MO 64093.

[1]B. Vonnegut, J. Appl. Phys. **18**, 593 (1947).
[2]M. Volmer, *Kinetik der Phasenbildung* (Verlag, Dresden, 1939).
[3]N. H. Fletcher, *The Physics of Rainclouds* (Cambridge University Press, Cambridge, 1969), Chaps. 3 and 8; *The Chemical Physics of Ice* (Cambridge University Press, Cambridge, 1970), Chap. 4; J. Chem. Phys. **29**, 572 (1958); **31**, 1136 (1959); J. Met. **16**, 173 (1959); J. Chem. Phys. **13**, 408 (1960); J. Atmos. Sci. **26**, 1266 (1969).
[4]A review of classical homogeneous nucleation theory is given in F. F. Abraham, *Homogeneous Nucleation Theory* (Academic, New York, 1974).
[5]H. E. Gerber, J. Atmos. Sci. **33**, 667 (1976).
[6]N. H. Fletcher (unpublished).
[7]G. Vali (unpublished).
[8]H. R. Pruppacher and J. C. Klett, *Microphysics of Clouds and Precipitation* (Reidel, Boston, 1980), Chap. 9.
[9]A. C. Zettlemoyer, J. Colloid Interface Sci. **28**, 343 (1968); see also Ref. 8, pp. 255–257.
[10]P. V. Hobbs, *Ice Physics* (Clarendon, Oxford, 1974), pp. 522–523; for dipole moments see Chap. 1.
[11]N. H. Fletcher, J. Chem. Phys. **30**, 1476 (1959).
[12]R. Lacmann and I. N. Stranski, J. Cryst. Growth **13/14**, 236 (1972); T. Kuroda and R. Lacmann, *ibid.* **56**, 189 (1982).
[13]M. Faraday, Proc. R. Soc. (London) **10**, 440 (1860), B. Beaglehole and D. Nason, Surf. Sci. **96**, 357 (1980) measure the coefficient of ellipticity for the basal and prism faces of ice and report a liquidlike layer on the prism face for temperatures as low as −5 °C and a liquidlike layer on the basal face near 0 °C; see also Refs. 1–5 in B. Beaglehole and D. Nason.
[14]S. Mantovani, S. Valeri, A. Loria, and U. del Pennino, J. Chem. Phys. **72**, 1077 (1980).
[15]Y. Mizuno and N. Hanfusa, J. Phys. (Paris) Colloq. **48**, C1-511 (1987).
[16]Y. Furukawa, M. Yamamoto, and T. Kuroda, J. Cryst. Growth **82**, 665 (1987).
[17]A. Kouchi, Y. Furukawa, and T. Kuroda (unpublished).
[18]B. Jönson, Chem. Phys. Lett. **82**, 520 (1981).
[19]M. Marchesi, Chem. Phys. Lett. **97**, 224 (1983).
[20]C. Y. Lee, J. A. McCammon, and P. J. Rossky, J. Chem. Phys. **80**, 4448 (1984).
[21]N. B. Parsonage and D. Nicholson, J. Chem. Soc. Faraday Trans. 2 **82**, 1521 (1986); **83**, 663 (1987).
[22]J. P. Valleau and A. A. Gardner, J. Chem. Phys. **86**, 4162 (1987); **86**, 4171 (1987).
[23]E. Spohr and K. Heinzinger, Chem. Phys. Lett. **123**, 218 (1986); Chem. Phys. **141**, 87 (1990); E. Spohr and K. Heinzinger, Ber. Bunsenges. Phys. Chem. **92**, 1358 (1988).
[24]E. Spohr and K. Heinzinger, Electrochim. Acta **33**, 1211 (1988).
[25]G. Aloisi, M. L. Foresti, and R. Guidelle, J. Chem. Phys. **91**, 5592 (1989); G. Aloisi and R. Guidelle, *ibid.* **95**, 3679 (1991).
[26]J. Hautmann, J. W. Halley, and Y-J. Rhee, J. Chem. Phys. **91**, 467 (1989).
[27]E. Sphor, J. Phys. Chem. **93**, 6171 (1989).
[28]K. Heinzinger (unpublished).
[29]V. V. Ilyin, V. M. Khryapa, and N. V. Churaev, Ukranian Institute for Theoreticla Physics Report No. 89-35 (unpublished).
[30]S. B. Shu and G. W. Robinson, J. Chem. Phys. **94**, 1403 (1991).
[31]K. Foster, K. Raghavan, and M. Berkowitz, Chem. Phys. Lett. **162**, 32 (1989); K. Raghavan, K. Foster, K. Motakabbir, and M. Berkowitz, J. Chem. Phys. **94**, 2110 (1991).
[32]B. N. Hale and J. Kiefer, J. Chem. Phys. **73**, 923 (1980).
[33]R. C. Ward, J. M. Holdman, and B. N. Hale, J. Chem. Phys. **77**, 3198 (1982).
[34]B. N. Hale, J. Kiefer, S. Terrazas, and R. C. Ward, J. Phys. Chem. **84**, 1473 (1980).
[35]R. C. Ward, B. N. Hale, and S. Terrazas, J. Chem. Phys. **78**, 420 (1983); B. N. Hale and R. C. Ward, J. Stat. Phys. **28**, 487 (1982).
[36]S. Terrazas, Ph.D. dissertation, Department of Physics, University of Missouri-Rolla, 1983. In this study water monolayer clusters on a smooth Lennard-Jones substrate appear to be "liquidlike" at 265 K, and composed of fluctuating five- and six-membered rings.
[37]F. H. Stillinger and A. Rahman, J. Chem. Phys. **68**, 666 (1978).
[38]For other effective pair potentials for water see Refs. 5, 8, 12, 22, 41, 43, and 44 of M. D. Morse and S. A. Rice, J. Chem. Phys. **76**, 650 (1982); A. C. Belch and S. A. Rice, *ibid.* **78**, 4817 (1983); G. Nielson and S. A. Rice, *ibid.* **78**, 4824 (1983);

M. Wocjik and E. Clementi, *ibid.* **85**, 6085 (1986), and references therein; W. L. Jorgensen, J. Chandrasekhar, J. D. Madura, R. W. Impey, and M. L. Klein, *ibid.* **79**, 926 (1983); R. W. Impey, M. L. Klein, and J. S. Tse, *ibid.* **81**, 6406 (1984), and references therein; P. Barnes, in *Progress in Liquid Physics,* edited by C. A. Croxton (Wiley, Chichester, 1978); W. K. Lee and E. W. Prohofsky, *ibid.* **75**, 3040 (1981); W. J. Jorgenson, *ibid.* **77**, 4156 (1982); H. L. Nguyen and S. A. Adelman, *ibid.* **81**, 4564 (1984); K. T. Tang and J. P. Toennies, *ibid.* **80**, 3738 (1984); J. H. Lin and B. J. Garrison, *ibid.* **80**, 2904 (1984), J. E. Muller and J. Harris, Phys. Rev. Lett. **53**, 2493 (1984); M. W. Ribarsky, W. D. Luedtke, and U. Landman, Phys. Rev. B **32**, 1430 (1985).

[39]P. W. Deutsch, B. N. Hale, R. C. Ward, and D. A. Reago, Jr., J. Chem. Phys. **78**, 5103 (1983); P. W. Deutsch, B. N. Hale, R. C. Ward, and D. A. Reago, J. Phys. Chem. **87**, 4309 (1983).

[40]K. Han and B. N. Hale, Phys. Rev. B **45**, 29 (1992).

[41]The Ewald sum follows that used by M. J. Sangster and M. Dixon, Adv. Phys. **25**, 247 (1976).

[42]We note that a small mismatch between the dimensions of the water unit cell parallel to the plane of the substrate and the periodicity of the substrate exists. This causes a small discrepancy ($<0.1\%$ of the total surface potential interaction) in the water-substrate interaction when a molecule leaves the simulation volume on one side and returns on the other. In all cases the water-substrate interaction for a periodically translated molecule is recalculated before the accept-reject decision is made.

[43]M. Metropolis, A. Rosenbluth, M. Rosenbluth, A. Teller, and E. Teller, Phys. A **21**, 1087 (1953). Our particular method for the treatment of (rigid) water molecules is adapted from J. A. Barker and R. O. Watts, Chem. Phys. Lett. **3**, 144 (1969). See also K. Binder, in *Monte Carlo Methods in Statistical Physics,* edited by K. Binder (Springer-Verlag, Berlin, 1979), Chap. 1.

[44]H. K. Christenson and J. N. Israelachvili, J. Chem. Phys. **80**, 4566 (1984); **88**, 7162 (1988).

[45]S. Toxvaerd, Faraday Sympos. **16**, 1 (1981); J. Chem. Phys. **74**, 1998 (1981); L. F. Rull and S. Toxvaerd, *ibid.* **78**, 3273 (1983).

[46]J. C. Owicki and H. A. Scheraga, Chem. Phys. Lett. **47**, 600 (1977).

[47]J. A. Kerr and J. Kiefer, J. Chem. Phys. **89**, 4313 (1988).

[48]For a description of the structure factor calculation see Eqs. (1)–(3) in Ref. 40. In Fig. 2 of Ref. 40 the two lattice vectors in the xy plane are shown. In the present work $S_i = N^{-2}|\sum_{j=1,N}\exp(i\mathbf{k}_1\cdot\mathbf{r}_j)|^2$.

[49]R. A. Bakhanova and V. I. Kiselev, Kolloidn. Zh. **34**, 481 (1972); **36**, 747 (1974) [Colloid J. U.S.S.R **34**, 481 (1972); **36**, 680 (1974)].

[50]F. Franks, in *Water: A Comprehensive Treatise, Vol. 7,* edited by F. Franks (Plenum, New York, 1982), p. 242.

[51]P. V. Hobbs, *Ice Physics,* Ref. 10, pp. 504–512.

[52]N. H. Fletcher, Philos. Mag. **7**, 255 (1962); **8**, 1425 (1962).

[53]R. M. Townsend, J. Gryko, and S. A. Rice, J. Chem. Phys. **82**, 4391 (1985).

[54]K. W. Kehr and K. Binder, in *Applications of the Monte Carlo Method in Statisical Physics,* edited by K. Binder (Springer-Verlag, New York, 1984), p. 184.

[55]J. Kiefer (private communication). A longer run was made on the bulk H_2O system of Ref. 47 at $T=330$ K for a total of 3.65×10^{-12} sec. The data give a diffusion coefficient $=(0.7\pm0.1)\times10^{-5}$ cm^2/sec.

[56]R. Mills, J. Phys. Chem. **77**, 685 (1973); K. T. Gillen, D. C. Douglas, and M. J. R. Hoch, J. Chem. Phys. **57**, 5117 (1972). Taken from Fig. 19, p. 44 of C. A. Angell, in *Water, A Comprehensive Treatise,* edited by F. Franks (Plenum, New York, 1982).

[57]R. O. Ramseier, J. Appl. Phys. **38**, 2553 (1967).

[58]D. Nenow, J. Cryst. Growth **9**, 185 (1984).

[59]D-M. Zhu and J. G. Dash, Phys. Rev. Lett. **57**, 2959 (1986).

[60]J. X. Larese and Q. M. Zhang, Phys. Rev. Lett. **64**, 922 (1990).

[61]J. W. M. Frenken and J. F. van der Veen, Phys. Rev. Lett. **54**, 134 (1985); J. W. M. Frenken, P. M. J. Maree, and J. F. van der Veen, Phys. Rev. B **34**, 7506 (1986); P. H. Guoss and L. J. Norton, Phys. Rev. Lett. **60**, 2046 (1988).

[62]R. M. J. Cotterill, Philos. Mag. **32**, 1283 (1975); J. K. Kristensen and R. M. J. Cotterill, *ibid.* **36**, 437 (1977).

[63]J. Q. Broughton and L. V. Woodcock, J. Phys. C **11**, 2743 (1979).

[64]V. Rosato, G. Ciceotti, and V. Pontikis, Phys. Rev. B **33**, 1860 (1986).

[65]J. Q. Broughton and G. H. Gilmer, J. Chem. Phys. **79**, 5095 (1983); **79**, 5105 (1983); **79**, 5119 (1983); G. H. Gilmer and J. Q. Broughton, J. Vac. Sci. Technol. B **1**, 298 (1983).

[66]A. L. Cheng and W. A. Steele, Langmuir **5**, 2036 (1990).

[67]P. Stoltze, J. Chem. Phys. **92**, 6306 (1990).

[68]R. Montmory (private communication); see also R. Montmory, Bull. Obs. Puy de Dome, Ser. 2, No. 4, 126 (1956).